J. Membrane Biol. 125, 25–39 (1992)

The Journal of
Membrane Biology

Chara Plasmalemma at High pH: Voltage Dependence of the Conductance at Rest and during Excitation

Mary J. Beilby† and Mary A. Bisson‡

†School of Biological Sciences, University of Sydney, NSW 2006, Australia, and ‡State University of New York at Buffalo, Buffalo, New York 14260

Summary. The high pH state of *Chara* plasmalemma (Bisson, M.A., Walker, N.A. 1980. *J. Membrane Biol.* **56:**1–7) was investigated to obtain detailed current-voltage (I/V) and conductance-voltage (G/V) characteristics in the pH range 7.5 to 12. The resting conductance started to increase at a pH as low as 8.5, doubling at pH 9.5, but the most notable increases occurred between pH 10.5 and 11.5, as observed previously (Bisson, M.A., Walker, N.A. 1980. *J. Membrane Biol.* **56:**1–7; Bisson, M.A., Walker, N.A. 1981. *J. Exp. Bot.* **32:**951–971). The slopes (and shapes) of the I/V curves varied even over minutes, suggesting a shifting population of open channels. Possible contributions of the permeabilities to H^+ and OH^-, P_H and P_{OH}, respectively, to the increase in membrane conductance were calculated in the pH range 8.5 to 12. If P_H is the main cause for the increase in conductance, it would have to rise by three orders of magnitude between pH 8.5 and 11.5, implying an enormous increase in the open-channel population as pH rises. On the other hand, a comparatively constant P_{OH} over that pH range would result in an increase in conductance due to the rise of OH^- concentration. This indicates unchanging open-channel population.

The transient excitation conductances at pH 7.5 and 11.5 were compared at a range of membrane PD (potential difference) levels. At more positive PD levels (near 0) the transient conductances showed little change as pH was increased. However, near the excitation threshold the conductance at high pH was slower to reach peak and its amplitude was diminished compared to that at neutral pH. This effect was found to be partially due to the pH change itself and partially due to less negative membrane PD at high pH. The changes in excitation transients developed gradually as pH of the medium was increased. These findings are discussed with a recent model of excitation in mind (Shiina, T., Tazawa, M. 1988. *J. Membrane Biol.* **106:**135–139).

Key Words *Chara* · current-voltage analysis · high pH state · excitation transients · cytoplasm-enriched fragments

Introduction

The high pH state highlights the enormous versatility of the plant plasmalemma: not only can the cell survive the hostile environment of pH up to 12, it utilizes this state in the banding system to assimilate carbon and to control cytoplasmic pH (Walker, Smith & Cathers, 1980; Lucas 1982, 1985; Price & Badger, 1985). The high pH state has been well documented only in the *Characeae* (Bisson & Walker, 1980, 1981, 1982), but is presumed to exist in other systems, such as aquatic angiosperms (Prins et al., 1980). In a recent article Raven (1991) surveyed rhizophytes from many habitats, which exhibit H^+-borne circulating currents (and consequently acid and alkaline zones). The high pH channels might therefore be more widely spread through the plant kingdom than previously suspected.

The high pH state manifests itself by high conductance (up to 20 $S \cdot m^{-2}$) and pH electrode-like behavior of the resting PD (Bisson & Walker, 1980, 1982). However, the latter does not always accompany the former (Bisson & Walker, 1981). Bisson and Walker (1980) attempted to differentiate whether the permeant ion is H^+ or OH^-. In this paper we extend their considerations by recording I/V characteristics for the plasmalemma at rest over pH range 7.5 to 12. What information can we obtain from such data? Voltage dependence is often a distinct characteristic for a particular type of channel. Further, we record the I/V profile in a minimally perturbed cell. The patch-clamp technique, on the other hand, often involves extensive disturbance to the system under study (Gradmann, 1989). The giant-celled algae are no exception. Coleman (1986) used sharp scissors to cut the cell wall of a partially plasmolyzed *Chara* cell to access an exposed plasmalemma. This line of enquiry was then neglected (perhaps due to the great ease of working on cytoplasmic drops bound by tonoplast) until Laver (1991) improved the Coleman technique by employing a special tool to cut a window in the cell wall. The high pH channels are more sensitive to manipulations (compared to the proton pump or the K^+ channels), as their conductance is abolished by cytoplasmic perfusion (Lucas & Shimmen, 1981). The future patch-clamp experiments thus might not show the

normal in vivo characteristics, and our data will provide a useful comparison.

The *I/V* characteristics can also yield the conductance (and permeability), which enables us to predict the behavior of channel populations if the permeant ion is H^+ or OH^-.

The other aim of this paper is to describe the action potential at high pH. Excitation transients were known to occur when the cell was in high pH medium (Beilby, 1989*a*), but the detailed behavior was not investigated. We fill this gap in our knowledge of the high pH state. The results are analyzed with the new picture of excitation in mind (Shiina & Tazawa, 1987*a,b*, 1988).

Materials and Methods

Chara corallina was used for the experiments, either as intact cells or as cytoplasm-enriched fragments. The experiments were performed in Buffalo, New York, and Sydney, NSW, Australia. In 1981 MAB observed unusually shaped action potentials, which inspired further investigation using voltage clamp. The experiments were performed in July 1988 by MAB and MJB in Sydney. Some of the data were published by Beilby and Shepherd (1989), comparing behavior of fragments and intact cells at high pH. More experiments were done between November 1988 and January 1989 by MJB.

In Buffalo the *Chara* cells were obtained from R.M. Spanswick and grown in Broyer and Barr medium, as detailed in Bisson and Bartholomew (1988). During experimental procedures the cells were bathed in APW (0.2 or 2.0 mM K_2SO_4, 1.0 mM NaCl, 0.1 mM $CaCl_2$, 5 mM HEPES, pH 7, 5 mM CAPS, pH 11). The electrophysiological apparatus consisted of WPI F-23A electrometer, Grass stimulator and Gould recorder. The current was point injected through a glass micropipette, and the PD measuring electrode was placed in the vacuole (*see* for instance Bisson & Walker, 1980). Low amplitude current pulses were injected at the time of the action potential (AP) to estimate the cell conductance.

In Sydney the cells came from laboratory tanks, glasshouse tanks or outdoor tanks (for more details on origins of these cultures *see* Beilby, 1990*a*). The growth media were not controlled. The experimental APW consisted of 0.1 mM KCl, 1.0 mM NaCl, 0.5 mM $CaCl_2$, 1 mM appropriate Good buffer and NaOH. In the pH range 7.5 to 11.0, less than 5 mM NaOH was necessary to bring the APW to desired pH value. Above pH 11.0, no biological buffer was available with sufficiently high pK. The amounts of NaOH ranged from about 7 mM at pH 11.5 to up to 30 mM at pH 12.0. The effect of Na^+ on the *I/V* characteristics was tested by adding 2.5–15 mM Na_2SO_4 at pH 10.5. All the solutions were made fresh before each experiment and passed over the cell with fast flow rates. Initially in the joint MAB and MJB experiments, the rate was 10 ml/1.5 min, but later this was increased to 10 ml/12 sec. The reasons for this are discussed in Results. The volume of the experimental chamber was 2 ml. The cells were illuminated by a fiberoptics light source at all times.

While there are definite seasonal variations (Shepherd & Goodwin, 1991), all intact cells showed pump states (that is negative PD below −200 mV near neutral pH, *see* Beilby & Shepherd, 1989; and Fig. 1*A*). The fragments tended to be less hyperpolarized, but that was generally found to be the case (Beilby & Shepherd, 1989).

The apparatus has been described in detail previously (Beilby & Beilby, 1983; Beilby, 1990*a*). Briefly, the cells and fragments were space clamped by passing a wire along their axes. They were voltage clamped to computer-generated commands: bipolar staircase for *I/V* curves and longer (seconds) step changes in potential with superimposed sine wave for the excitation studies. The clamp current and the cell PD were data logged by the computer at a rate of 1 point/msec. The *I/V* curves were obtained by plotting the average of the last 10 data points from each current and potential pulse, respectively. The *G/V* curves were calculated by fitting a polynomial to the *I/V* curves, three points at a time, and differentiating. The time dependence of the response of the cell current at high pH to the bipolar staircase command was investigated previously (Beilby, 1990*a*). The procedure for the calculation of the conductance (impedance) from the sine wave and the step change in potential clamp command is described in detail in Beilby and Beilby (1983).

To determine whether the changes in excitation are due to depolarization of the resting PD or directly due to changes of the pH_o (and probably pH_{cyt}), we tried to clamp the cells in the high pH state to a hyperpolarized PD. However this resulted in large currents across the conductive membrane, which in turn proved to be deleterious to the cell. Consequently, we adopted the procedure of depolarizing the cells at neutral pH to PDs usually observed at pH 11.0 (typically −150 mV in the first 30 min). This "preclamp" was maintained for up to 30 min. Every 5 min the membrane PD was clamped to some excitatory level with superimposed sine wave.

To obtain a free running action potential (AP), the membrane PD was clamped to a level sufficiently depolarized to elicit excitation. The clamp was manually switched off allowing the membrane PD to drift freely. The depolarizing stage of the AP was often lost, as it was difficult to judge if the threshold had been reached.

Results

Transition into High pH State

In previous experiments Bisson and Walker (1980, 1981) generally found fast transition into high pH state (occurring within a few seconds), regardless of whether the cells started from the pump state or K^+ state. Beilby (1986*b*) observed a different type of behavior while working on cells in Cambridge, England. The plasmalemma conductance dropped considerably at first, then increased to the values generally encountered in the high pH state. The process took up to 1 hr. In the experiments reported here we encountered the latter type of transition, when a low rate of flow of external solutions was employed. Figure 1*A* and *B* show the *I/V* and *G/V* curves in the pump state, low *G* state as the high pH APW was slowly introduced into the cell chamber and finally the high pH state. The shading shows the difference curve for the pump state and low *G* state. When high

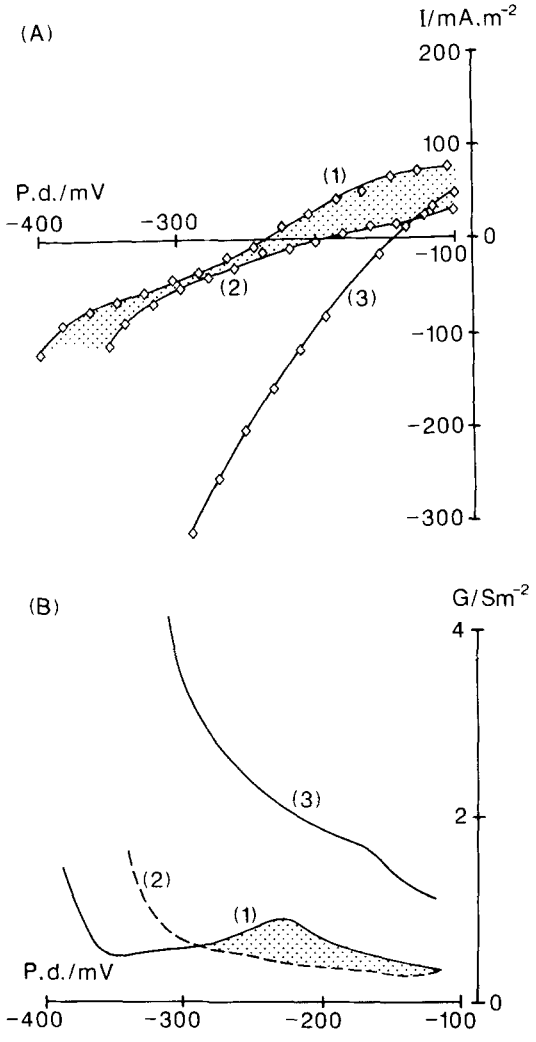

Fig. 1. (*A*) Transition of the plasmalemma *I/V* profile (intact cell) into the high pH state, as the cell is irrigated slowly with APW adjusted to pH 11.5. Curve *1* was recorded after the cell stabilized in the pump state, *2* after 30 min of slow flow APW, pH 11.5; at 5 min after recording of curve *2*, curve *3* showed a fully developed high pH state. The shaded area shows the shape of the *DI/V* curve. *DI* is the difference between curve *1* and curve *2*. The lines are polynomials fitted to the data. (*B*) the *G/V* curves calculated from *A*. The conductance for *I/V* profile *2* is shown as a broken line. The shaded area again shows *DG/V* for the transition state. *DG* is the difference in conductance calculated from the *I/V* curves *1* and *2*.

flow rate was used, the fast transition into the high pH state was always observed.

I/V and *G/V* Profiles in the Basic pH Window

Data comparing the *I/V* and *G/V* profiles in the pump state and the high pH state for intact cells and cytoplasm-enriched fragments have been published already (Beilby & Shepherd, 1989, Figs. 6 and 7, respectively) and are not repeated here. These data showed minor differences between fragments and intact cells particularly at high pH. Thus in this present study the data from intact cells and fragments were pooled.

Figure 2*A* shows the *I/V* curves for the pH range 7.5 to 11.5. The extremes of pH 12 and 4.5 (for completeness) are shown separately in Fig. 2*C* for clarity. The appropriate *G/V* profiles (for computation *see* Materials and Methods) are shown in Fig. 2*B* and *D*, respectively. Note the simple profiles of the *I/V* curves at and above pH 10.5, almost a straight line, with only a slight downward concavity. At pH 10.5 and 11.5 the conductance trend indicated some decrease at PDs more positive than −100 mV (*see* Figs. 2 and 3—but in Fig. 2 the large oscillation at PDs more positive than −100 mV, in the 10.5 pH *G/V* curve probably reflects the variability of the data rather than real conductance trend). At PDs more positive than −50 mV the rise of rectifier current dominated the *I/V* characteristics. Note also the doubling of the resting conductance at pH 9.5. The error bars were large at the extremes of the PD window. This effect was due to large variability of the rectifier currents and the *I/V* profiles at the high pH. Note also that at pH 11.5 the experiments described by Beilby and Shepherd (1989) yielded a resting PD of about −150 mV in both intact cells and fragments. The cell and fragment data shown in Fig. 2 averaged resting PDs of −170 (±12) mV at pH 10.5 and −182 (±12) mV at pH 11.5. Some fragments, such as the one shown in Fig. 3, hyperpolarized to PDs more negative than −200 mV at pH 11.5 and remained steady for at least 20 min. The profiles in Fig. 3 illustrate some of the diversity of behavior contained within the averaged data of Fig. 2: the conductance rose more steadily between pH 9.5 and 11.5. Some insight can also be gained into the behavior of the inward and outward rectifiers, as pH increased: both tend to be shifted to the more depolarized PDs. The inward-rectifier current is carried by Cl^- (Tyerman, Findlay & Paterson, 1986*a*). However, Tyerman et al. (1986*b*) found that an increase in pH shifts the onset of this current to more hyperpolarized PDs—the opposite to our observations. The outward rectifier is probably carried by an outflow of K^+, but the detailed dynamics have yet to be investigated.

The *I/V* profiles of the fragment in Fig. 3 were comparatively steady. In Fig. 4 *I/V* curves at pH 11.5 from another fragment (from the same batch) demonstrate how variable the conductance can be. The response also depended on the order of pH

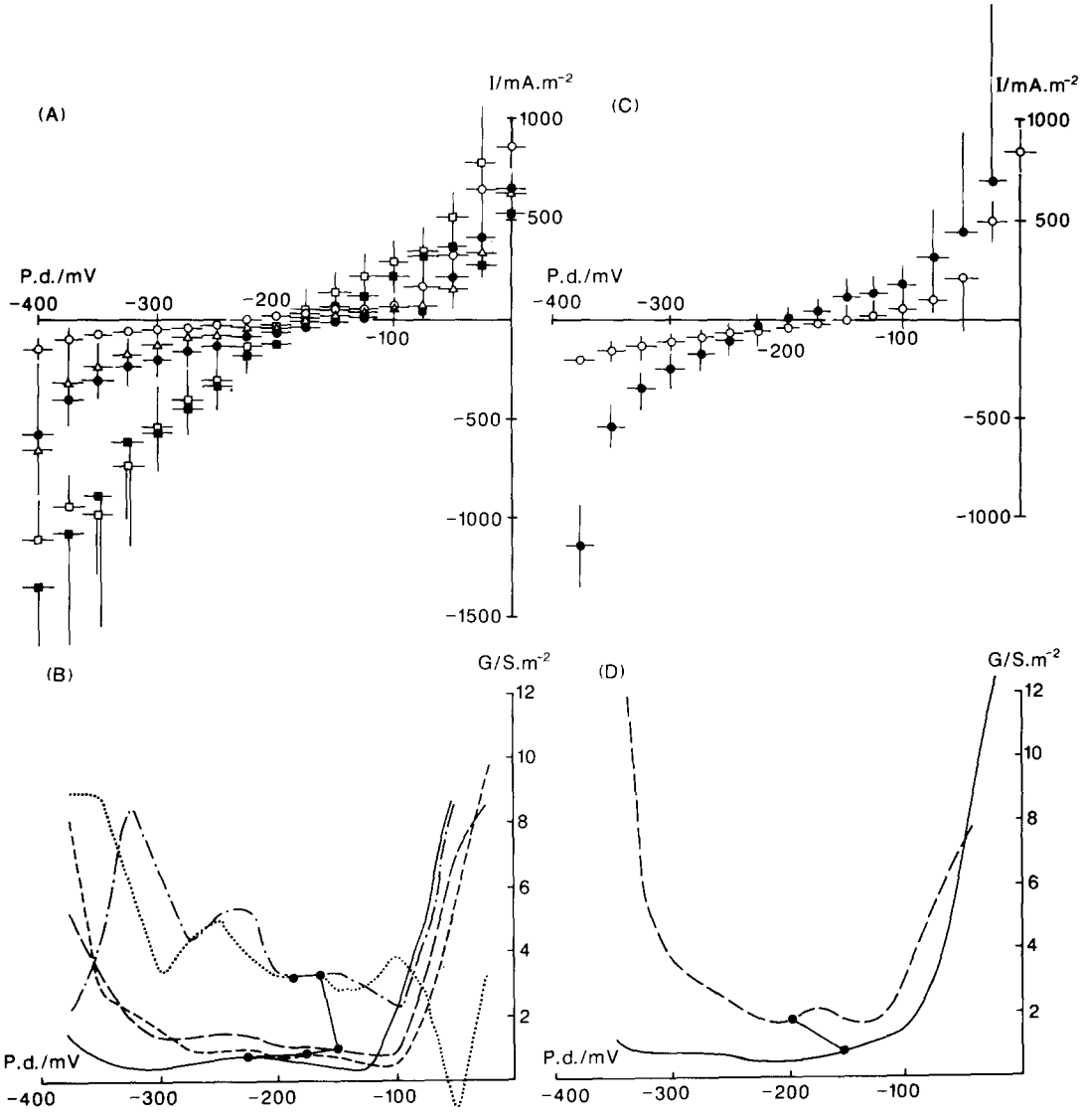

Fig. 2. Statistical treatment of the experimental data. (*A*) *I/V* curves for pH values 7.5 (○, three intact cells and two fragments), 8.5 (△, four cells and two fragments), 9.5 (●, two fragments and two cells), 10.5 (■, two cells and two fragments) and 11.5 (□, two fragments and two cells). The data were sorted into 25-mV bins indicated by horizontal bars; the vertical bars show the standard error. (*B*) the *G/V* profiles calculated from *A* as described in Materials and Methods: pH 7.5 (———), 8.5 (– – – – –), 9.5 (— — — —), 10.5 (·····), and 11.5 (–·–·–). The resting PD is indicated on each curve as a dot, and these dots are linked in order of increasing pH. (*C*) The data for pH 12 (●, two cells, two fragments, five *I/V* runs) are shown separately for reasons of clarity, and data from the other pH extreme of 4.5 (○) are included for completeness (five cells). Data are processed as in *A*. (*D*) The *G/V* profiles calculated from *C*: pH 12 (– – – –) and 4.5 (——).

values presented to the cell: the *I/V* at pH 9.5 was steeper following pH 11.5 than before. Note that this behavior was seen in the fragments, where it is not likely to be due to changes of cytoplasmic pH (the fragments have the same surface area as intact cells, but much greater mass of cytoplasm).

An addition of 10–30 mM Na^+ to the APW at pH 10.5 resulted in an unexpectedly complex response. The resting PD depolarized by 10 to 20 mV. At PD levels more negative than −300 mV all cells developed large negative currents. If the cells were depolarized to PD levels more positive than −100 mV, large positive currents resulted and the cell became depolarized for long times. Such behavior was observed before (Beilby, 1985). In the vicinity of the resting potential, some cells (three out of nine cells and fragments tested) became more conductive (*see* Fig. 5*A* and *B*), and others less conductive (*see* Fig. 5*C* and *D*). Either effect appeared immediately upon exposure to Na^+, but persisted to some extent

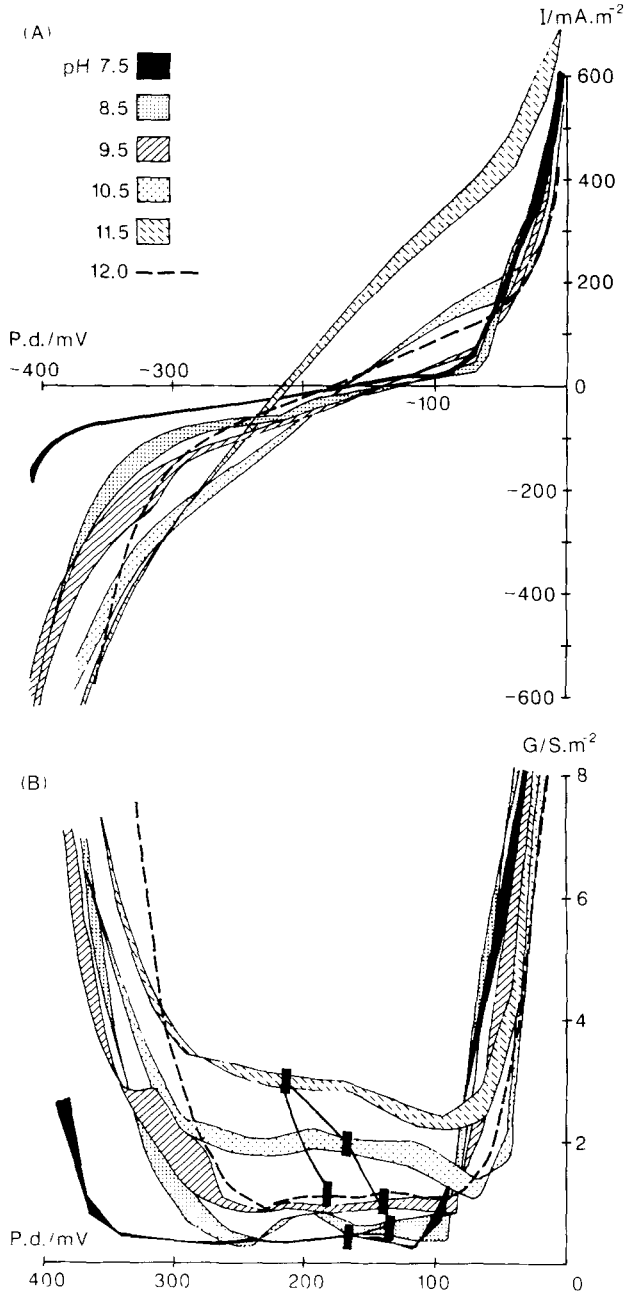

Fig. 3. Data from a cytoplasm-enriched fragment. (*A*) Two *I/V* profiles were data logged for each pH (except pH 12.0) within about 5 min. The two curves at the same pH are joined by shading those patterns that indicate the pH. Note the high resting PD at pH 11.5. (*B*) *G/V* curves calculated from *A*; same shading as in *A*. Note that the regions where conductance rises (due to inward and outward-rectifier currents) shift to more positive PDs as the pH rises. Resting PDs are indicated as in Fig. 2*B*, but in this case by rectangles.

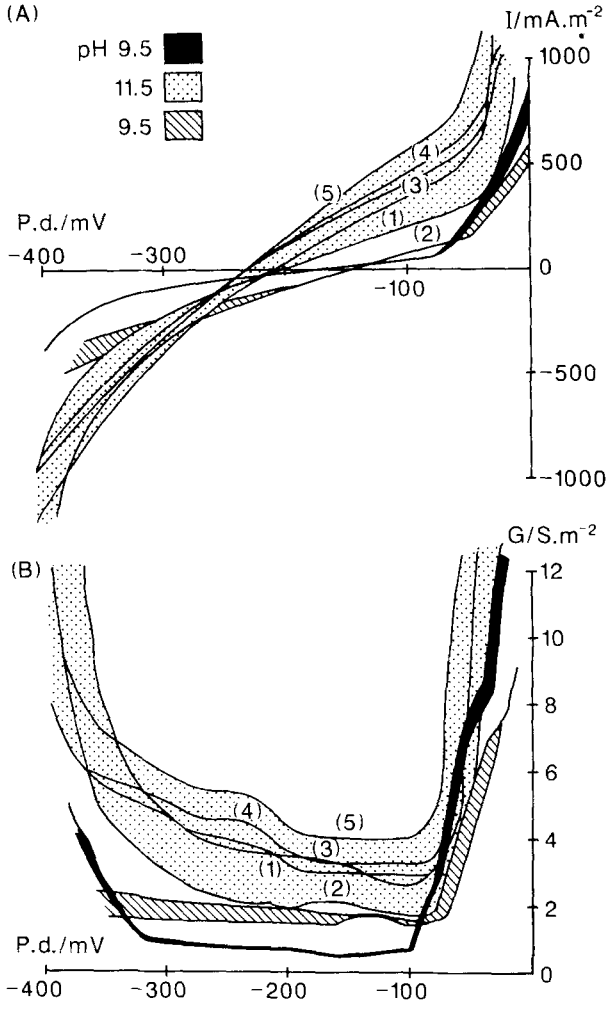

Fig. 4. The variability of the high pH *I/V* profile. In this experiment a different fragment to that in Fig. 3 was challenged with a range of pH values. (*A*) At pH 11.5 the profile was very variable, with both slope and resting PD changing over about 25 min. The curves are numbered in order of measurement. The *I/V* profiles were more stable at pH 9.5, but somewhat different depending on whether they were recorded before (black shading) or after (diagonal line) the fragment was exposed to pH 11.5. (*B*) The *G/V* profiles calculated from *A*.

after the Na_2SO_4 was washed out. In Fig. 5*A* and *B* a fragment showed a stable profile in pH 10.5. The *I/V* curve became steeper and the inward rectifier more pronounced as 10 mM Na^+ was added, but conductance fell when pH 12.0 was introduced into the chamber (the APW of pH 12.0 required an addition of 20 mM NaOH to achieve that pH value). The fragment survived overnight and the experiment was repeated, this time raising the Na^+ concentration to 20 mM. The conductance fell again at pH 12, but to a smaller extent. Figure 5*C* demonstrates that an addition of 5 mM Na^+ resulted in a shift too small to be significant within the variability of the high pH state. An exposure to 20 mM Na^+ diminished conductance in this cell (Fig. 5*D*). At the beginning of the experiment the cell was exposed to pH 11.5

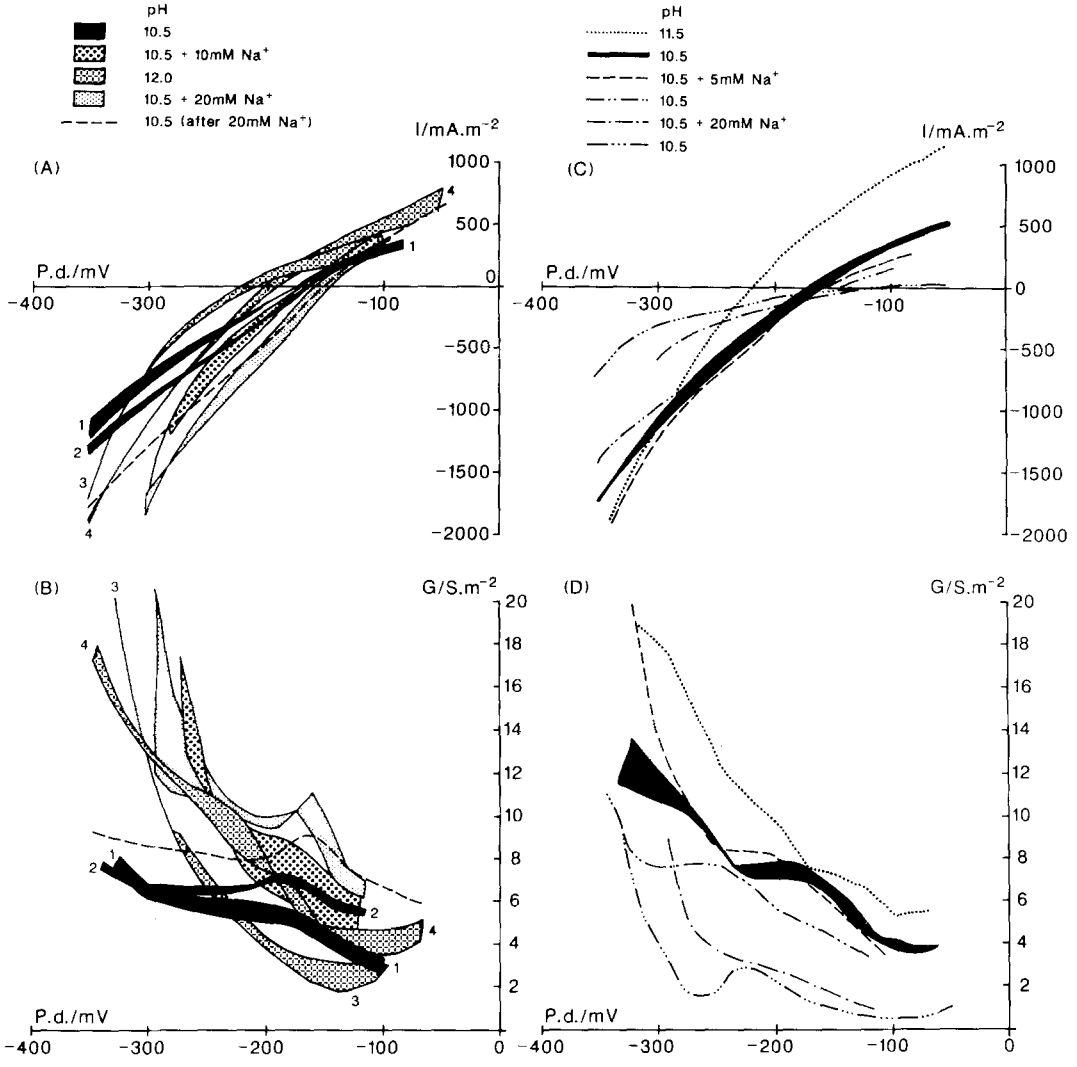

Fig. 5. The effect of Na^+ on the high pH state. (*A*) This experiment was performed on a cytoplasm-enriched fragment. The shading is delimited by two *I/V* curves obtained in quick succession within about 5 min. The conditions for each pair of *I/V* curves are given next to each pattern of shading. The sequence of solutions was as follows: pH 10.5 (*1*), pH 10.5 (*2*), pH 10.5 + 5 mM Na_2SO_4, pH 12 (*3*), pH 10.5 + 10 mM Na_2SO_4, pH 10.5 (in this case just a single *I/V* profile is shown as a dashed line), and pH 12 (*4*). All solutions at pH 10.5 were based on standard APW (*see* Materials and Methods). At pH 12, no buffer was used, and 20 mM NaOH was necessary to obtain this pH. (*B*) The *G/V* curves calculated from *A*; same shading applies. (*C*) This experiment was performed on an intact cell. The sequence of events was as follows: pH 11.5 (·····), pH 10.5 – two *I/V* runs in fast succession shown by shading, pH 10.5 + 2.5 mM Na_2SO_4 (– – – –), back to pH 10.5 (—·—·—·—), pH 10.5 + 10 mM Na_2SO_4 (—·—·—·—), and finally back to pH 10.5 (—·—·—·—·—). (*D*) The *G/V* profiles calculated from *C*.

(which required addition of 7 mM Na^+), and this *I/V* profile showed higher conductance than that at pH 10.5.

Excitation Transients

The cells in high pH state remained excitable, although in some Sydney experiments the excitability declined with time spent at high pH. Figure 6 shows action potentials from a *Chara* cell in 0.2 mM K^+ APW (Fig. 6*A* and *B*) and 2.0 mM K^+ APW (Fig. 6*C* and *D*). The experiment was performed in Buffalo. The increase in K^+ concentration changed the shape of the AP at the near neutral pH, and these changes were essentially preserved at pH 11.0. Note, however, that the shoulder (Fig. 6*C*) became a secondary peak (Fig. 6*D*).

In Fig. 7 action potentials are compared at pH 7.5 and 11.5. As explained in Materials and Methods, the Sydney experimental apparatus is not well suited to this function and the depolarizing phase is lost.

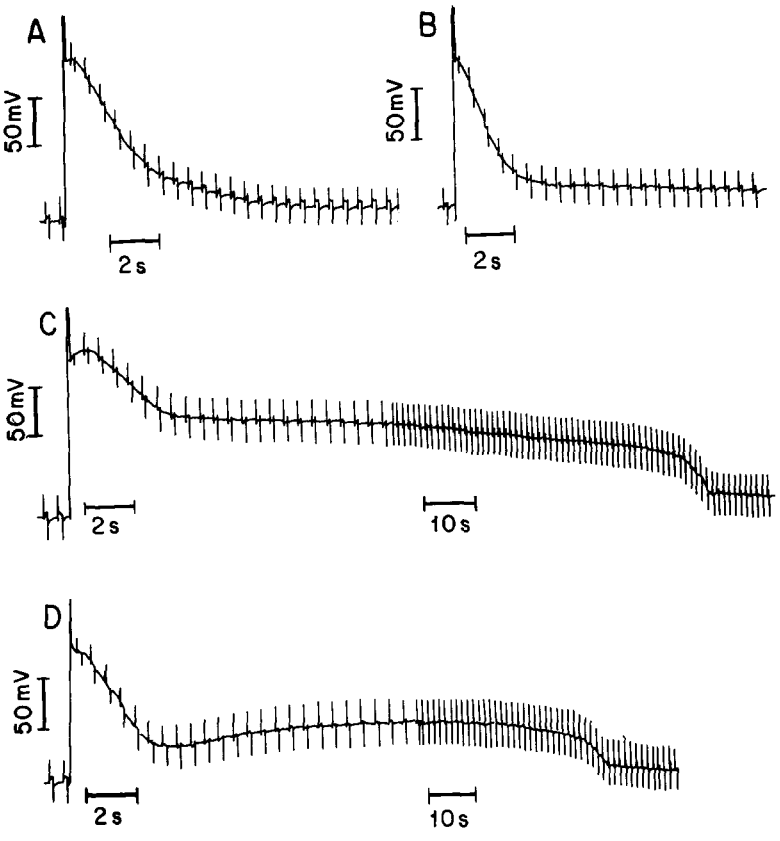

Fig. 6. Action potentials. (*A*) pH 7; 0.2 mM K^+; resting PD was −177 mV; resting conductance was 0.24 S · m^{-2}; conductance near the peak was 0.43 S · m^{-2}. (*B*) pH 11.0; 0.2 mM K^+; resting PD was −170 mV; resting conductance was 0.21 S · m^{-2}; conductance near the peak was 0.38 S · m^{-2}. (*C*) pH 7.0; 2.0 mM K^+; resting PD was −184 mV; resting conductance was 0.3 S · m^{-2}; conductance near the peak was 0.44 S · m^{-2}; conductance along the shoulder varied between 0.25 to 0.3 S · m^{-2}. (*D*) pH 11.0; 2.0 mM K^+; resting PD was −157 mV; resting conductance was 0.22 S · m^{-2}; conductance at the first peak was 0.42 S · m^{-2} and at the secondary peak was 0.25 S · m^{-2}. The experiment was performed in Buffalo, *see* Materials and Methods for apparatus details.

The initial rapid part of the repolarizing phase looks very similar at both values of pH (*see also* Fig. 4*A*, Beilby, 1989*a*).

In Fig. 8 excitation conductance transients at several clamp levels have been recorded at pH 7.5, 11.5 and finally back at 7.5. Note that there is a substantial decrease in amplitude at more negative PDs (−100 to −40 mV), with the more positive level transients remaining unchanged or even getting larger (Fig. 8*B*), but sometime decreasing upon return to pH 7.5. In general, at pH 11.0–11.5 the times to reach the peak conductance were longer and so were the times to settle into steady state (*see* Table 1 for statistics). At PDs more negative than −60 mV secondary peaks appeared more often than at neutral pH.

As mentioned in the previous section, the average resting PDs were more negative than those described by Beilby and Shepherd (1989). However, these resting PD levels were only observed while the cells were analyzed with the bipolar staircase voltage-clamp command. The more prolonged depolarization (up to 8 sec) to measure excitation transients brought the PD closer to −150 mV. We were interested whether depolarization also affected the conductance transients. The cells were depolarized by voltage clamping for periods of 5 to 15 min and

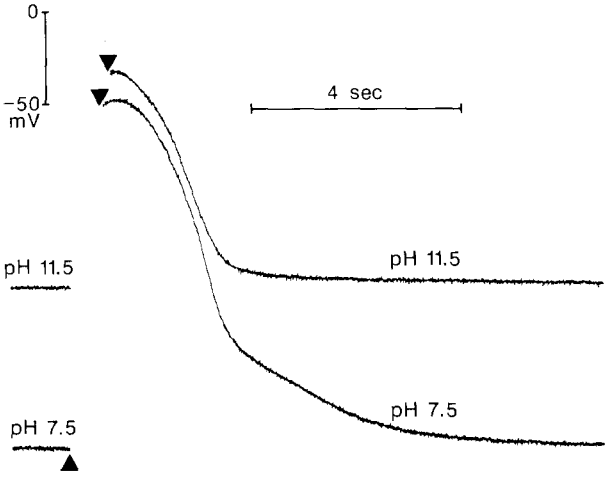

Fig. 7. Comparison of action potentials at pH 7.5 and 11.5. The apparatus is not well suited to measurement of free-running AP (*see* Materials and Methods for details), and the depolarizing phase is lost in this record. The PD was initially clamped to resting level, and then, at the upward arrow, the clamp level was changed to −50 mV (pH 7.5) and 0 PD (pH 11.5) and switched off mannually (downward arrows) to allow the membrane PD to drift. The electrode was placed in the cytoplasm prior to the recording, but had to be adjusted. It is possible that it moved into the vacuole, hence, the change of rate of repolarization after about 3 sec. The electrode was not moved between the recording of the two APs. The resting PD at pH 7.5 was −234 mV and at pH 11.5 was −148 mV. The experiment was performed in Sydney.

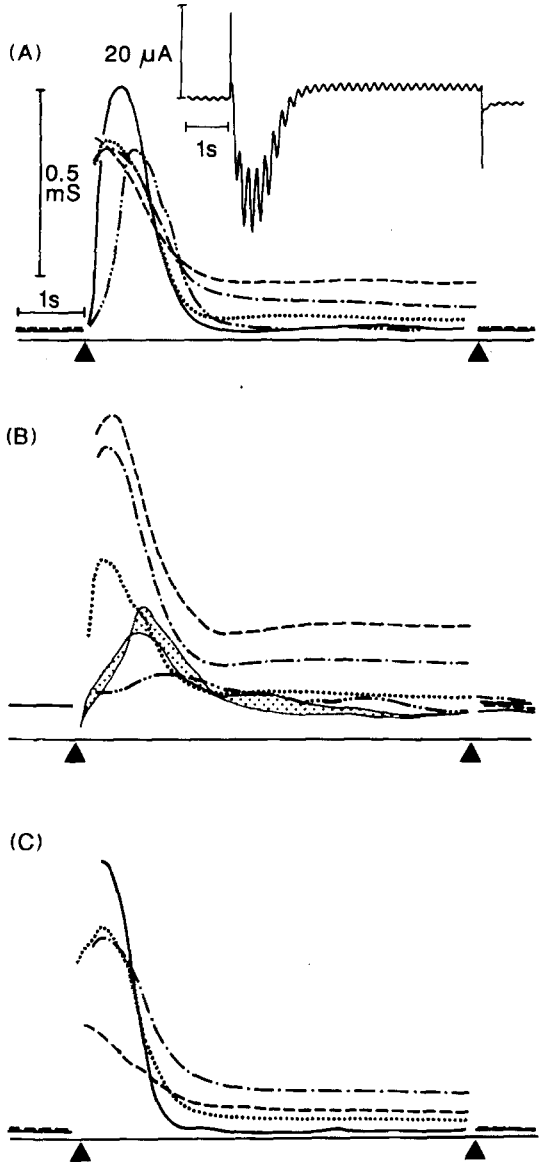

Fig. 8. The conductance transients at the time of excitation. The plasmalemma was voltage clamped to resting PD for 1 sec, then depolarized (upward arrow) to −100 mV (—·—·—·—·—·), −80 mV (———), −40 mV (·····), −20 mV (—·—·—·—·—) and 0 PD (– – – – –) for 5 sec, and finally back to resting level (upward arrow) for 1 sec. A sine wave of 10 mV and 5 Hz was superimposed on the clamp command, obtaining a record such as shown in the inset (for middle PD level of −40 mV). The conductance (or more correctly impedance) was calculated as described in Beilby and Beilby (1983). The area of the cell was 0.174 cm^2. The horizontal line at the bottom of each record indicates zero conductance. (*A*) pH 7.5; resting PD between −238 and −241 mV. (*B*) pH 11.5; resting PDs and times of each clamp level were: −100 mV (−168 mV and 36 min), −80 mV (−183 mV, 6 min at the first run, −167 mV and 31 min at the second time), −40 mV (−170 mV and 19 min), −20 mV (−169 mV and 26 min), and 0 PD (−176 mV and 13 min). (*C*) Cell returned to pH 7.5; resting PD between −236 and −242 mV. The 0 PD clamp was first to be performed.

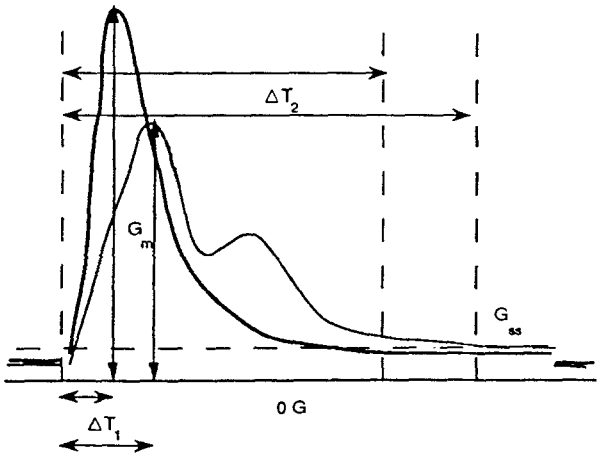

Fig. 9. Sketch of two conductance data sets, similar to those in Fig. 8. We define the maximum conductance, G_m; the time to reach the maximum, ΔT_1, and the time to arrive to a steady-state conductance G_{ss}, ΔT_2. In case of multiple peaks, the highest is taken as G_m, with ΔT_1 and ΔT_2 as before.

then put through the usual clamping protocol (Fig. 10). The experiments were performed in pump state, where the membrane is not very permeable and the long-term flow of current across the membrane did not seem to do any damage. Even so these were difficult experiments to perform, as the cytoplasmic electrodes tend to block in long-term clamping with fatal consequences to the cell (*see* Beilby, 1990*a*). In Fig. 10 it is apparent that the preclamp to −150 mV had similar effects to exposure to high pH: at negative levels such as −80 mV the transient conductance peak decreased in magnitude, but recovered after the preclamp was released; at more positive levels the effect was smaller, but the decrease remained after preclamp release. The secondary peaks also appeared. The results are summarized in Table 2 in a similar fashion as for the data in Table 1.

Finally we investigated whether the effect was a graded response to pH, or whether a sudden change could be observed at and above pH 10.5. Figure 11 shows that the excitation conductance transients gradually flattened out as pH increased. Interestingly, at pH 4.5 the more negative level transients were also more affected.

In the experiments involving transient currents the changes of Na^+ concentration were less important, as no measurements were performed at pH 12.0 and small increases in Na^+ concentration were found to have no effect on transient currents at pH 5.6 (Beilby & Coster, 1979*a*). Further, Bisson found that an addition of 10 mM Na^+ to APW at pH 10.5 had no effect on the shape of the action potentials (M.A. Bisson, *unpublished results*).

Table 1. Conductance at the time of excitation as function of pH[a]

PD (mV)	G_m (S · m^{-2})		G_{ss} (S · m^{-2})		ΔT_1 (sec)		ΔT_2 (sec)	
	11–11.5	7.5	11–11.5	7.5	11–11.5	7.5	11–11.5	7.5
20	32, 20	19	16, 12	12	0.7, 0.4	0.4	6, 4	5.4
0	28 ± 14 (6)	28 ± 5 (7)	10 ± 5	10 ± 2	0.7 ± 0.3	0.3 ± 0.1	5.0 ± 1.1	4.5 ± 1.0
−20	46, 44	28, 29	6, 11	6, 4	0.3, 0.4	0.2, 0.4	5.6, 3.6	4.6, 5.4
−40	14 ± 10 (8)	29 ± 11 (5)	4 ± 2	5 ± 2	1.3 ± 0.8	0.3 ± 0.1	5.5 ± 0.5	4.5 ± 1.2
−80	14 ± 4 (4)	30 ± 9 (7)	4 ± 0.5	4 ± 2	0.9 ± 0.1	0.4 ± 0.1	5.5 ± 0.3	4.9 ± 0.8
−110	9	18	4	1	1.3	0.6	6.0	4.0

[a] For definitions of G_m, G_{ss}, ΔT_1 and ΔT_2 refer to Fig. 9. For more than two measurements the results are given as the mean value ± SE. The number of measurements is given in brackets for G_m and is the same for the other parameters.

Table 2. Conductance at the time of excitation as a function of time the plasmalemma PD was preclamped to −150 mV[a]

PD (mV)	G_m (S · m^{-2})	G_{ss} (S · m^{-2})	ΔT_1 (sec)	ΔT_2 (sec)
0				
No preclamp	34 ± 6 (4)	9 ± 2	0.2 ± 0.05	3.6 ± 1.0
5 min	37	7	0.2	5.4
15 min	31, 26	3, 10	0.2, 0.3	3.7, 4.0
−20				
No preclamp	34 ± 10 (4)	5 ± 1	0.2 ± 0.1	4.4 ± 1.0
5 min	32	6	0.2	5.0
10 min	25	5	0.3	4.5
−40				
No preclamp	43 ± 12 (4)	3 ± 1	0.2 ± 0.1	3.1 ± 0.8
5 min	34, 33	3, 6	0.2, 0.6	4.3, 5.6
10 min	28	5	0.5	5.0
15 min	30	4	0.5	4.0
−80				
No preclamp	35 ± 4 (4)	2 ± 1	0.3 ± 0.04	3.8 ± 1.2
5 min	19 ± 8 (3)	1 ± 0.5	0.6 ± 0.3	5.2 ± 0.6
10 min	11, 14	1, 1	0.4, 0.4	3.6, 5.8
20–35 min	28 ± 10 (3)	2 ± 1	0.5 ± 0.03	4.9 ± 1.4

[a] G_m, ΔT_1, G_{ss} and ΔT_2 are defined as in Table 1. For more than two measurements, the results are given as the mean value ± SE. The number of measurements is given in brackets for G_m and is the same for the other parameters. See also Fig. 10.

Discussion

Transition into High pH State

While it was satisfying for us to identify the cause for the previously reported difference in time course of response when cells were challenged with high pH (i.e., the different rates of flow), the underlying changes in the plasmalemma transport remain obscure. Clearly, slowly incoming solution resulted in larger unstirred layers and possibly patches of different pH along the cell due to bad mixing. At first we assumed that we saw the shutting down of some system with a higher sensitivity to increased pH than that of the high pH channels. The K^+ transport was found to diminish markedly at high pH (Smith, Walker & Smith, 1987), and thus, seemed a likely candidate. However, the difference between the pump I/V curve and the transition state I/V (Fig. 1*A*) is very reminiscent of the pump inhibition, e.g., by cyanide (Blatt, Beilby & Tester, 1990). The G/V profiles confirm this opinion, as the conductance maximum believed to be generated by the proton pump (e.g., Hansen et al., 1981; Beilby, 1984) flattens out. Thus it seems that the pump is inhibited, as was originally assumed by Bisson and Walker (1980). This inhibition, however, is transient. Once

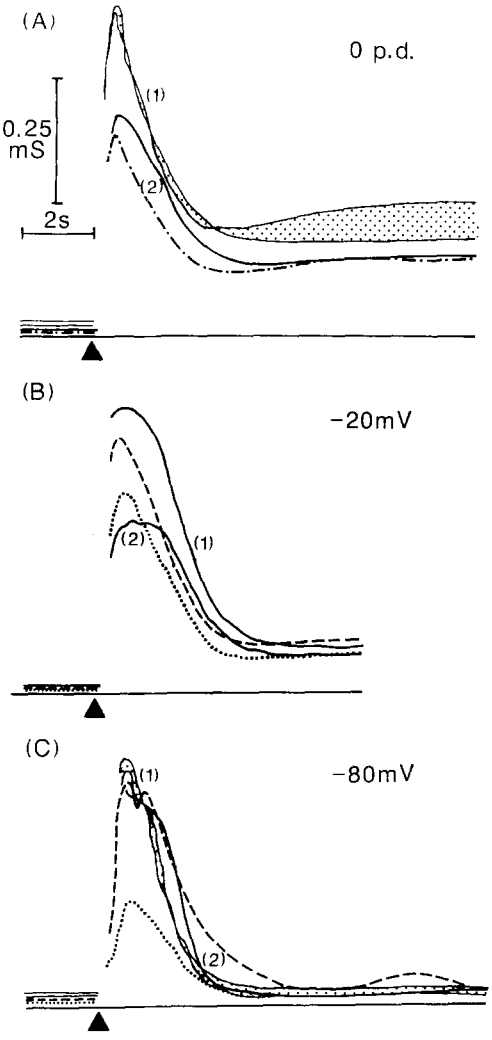

Fig. 10. The effect of depolarization on excitation conductance. The membrane was preclamped to −150 mV for 5 min (– – – – –), 10 min (·····) or 15 min (—·—·—·—), and then a protocol similar to that in Fig. 8 was imposed with excitatory PD levels at upward arrow (*A*) 0 PD, (*B*) −20 mV and (*C*) −80 mV (repolarization to resting PD *not shown*). In *A* only 15-min preclamp curve was recorded. The before (*1*) and after (*2*) transients are shown as continuous lines, or shaded areas (where the run was repeated to ensure reproducibility). The resting PD before preclamp was ~ −213 mV and returned to a value close to −240 mV within minutes of releasing the clamp. The cell area was 0.173 cm^2.

high pH state develops, the conductance maximum is often discernible again. This behavior was particularly apparent in Cambridge cells, which displayed strong pump currents (Beilby, 1984, 1986*b*) and to a smaller degree in the cell shown in Fig. 1*B* (a kink in curve (*3*) in the PD range −150 to −200 mV). If this PD range seems somewhat depolarized, it may be worth noting at this point that the models fitted to the pump *I/V* profile (Beilby, 1984; Blatt et al.,

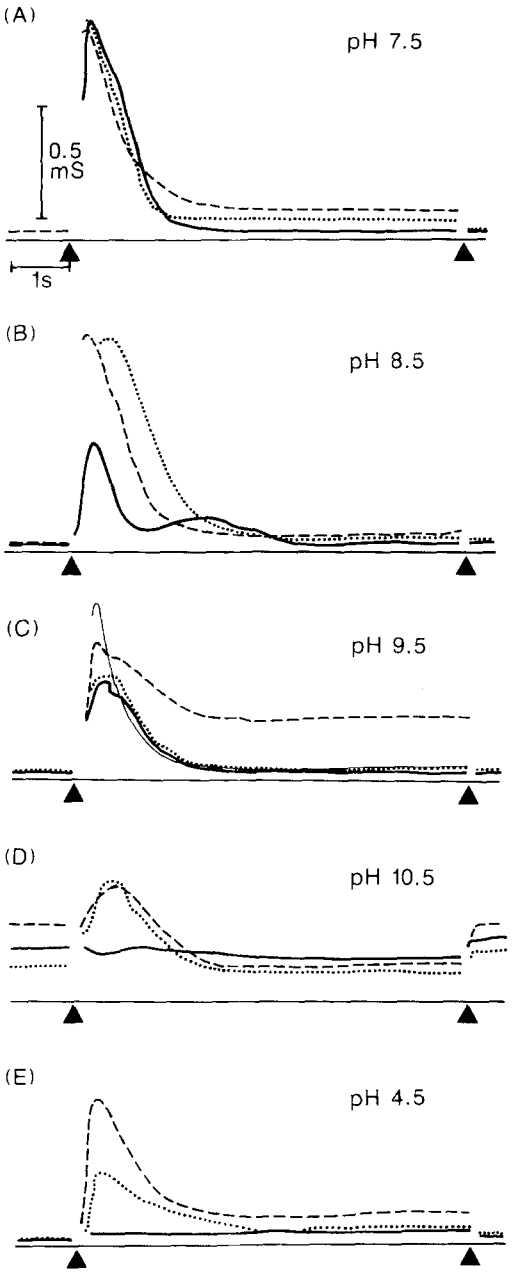

Fig. 11. The pH effect on excitation develops gradually as pH increases. The voltage-clamp protocol was as in Fig. 8 with excitatory PD levels at: 0 PD (– – – – –), −40 mV (·····) and −80 mV (———). (*A*) pH 7.5; resting PD −223 to −230 mV. (*B*) pH 8.5; since the resting PD shifted with time, we present here resting PD/excitatory PD (time): −158/−80 mV (19 min), −168/−40 mV (30 min), and −155 mV/0 PD (14 min). (*C*) pH 9.5; as in *B*: −167/−80 mV (12 min), −163/−40 mV (17 min), and −166 mV/0 PD (7 min). (*D*) pH 10.5; −167/−80 mV (12 min), −163/−40 mV (17 min), and −166 mV/0 PD (7 min). (*E*) pH 4.5; −121/−80 mV (14 min), −120/−40 mV (16 min), and −119 mV/0 PD (12 min). In *C* the thin continuous line shows transient at −80 mV, recorded at pH 7.5, which was introduced into the chamber between pH 9.5 and 10.5 for 10 min. In all cases the high pH was in the chamber for 30 min at most and cell was returned to pH 7.5 in between.

Table 3. Resting conductances and permeabilities due to H^+/OH^- channels as function of pH

pH	Resting PD E (mV)	$G_{<7.5}$ ($S \cdot m^{-2}$)	ΔG ($S \cdot m^{-2}$)	$E_{H/OH}$ (mV)	P_H ($m \cdot sec^{-1}$)	P_{OH} (10^{-4} $m \cdot sec^{-1}$)
4.5	−132	0.9	—	—	—	—
7.5	−225	0.8	—	—	—	—
8.5	−175	0.5	0.4	−40	0.03	1.5
9.5	−150	0.4	0.5	−98	0.2	1.3
10.5	−170	0.5	3.0	−155	5.8	2.9
11.5	−182	0.5	2.8	−213	10.1	0.5
12.0	−200	0.6	1.2	−241	8.0	0.1

The resting PDs were obtained from Fig. 2*A* and *C*. $G_{<7.5}$ gives the resting conductances at pH 7.5 and 4.5 (Fig. 2*B* and *D*). For other pH data, $G_{<7.5}$ provides the value on the *G/V* profile (pH 7.5) at resting PD for that pH. Thus total resting conductance at pH values above 7.5 is given by $G_{<7.5} + \Delta G$. For further details *see* text. To calculate the equilibrium potential for H^+/OH^-, the cytoplasmic pH was taken as 7.8, based on measurements by Reid and Smith (1988). The permeabilities P_H and P_{OH} were calculated from following equation:

$$P_H = \frac{\Delta G \cdot [\exp(zFE/RT) - 1]^2}{\frac{(zF)^2}{RT}[H^+]_o[[\exp(zF(E - E_H)/RT) - 1][\exp(zF/RT) - 1] + (zFE/RT)\exp(zF(E - E_H)/RT)[\exp(zFE_H/RT) - 1]]}$$

where z, F, R and T have their usual meanings. P_{OH} was calculated by substituting $[OH^-]_o$ for $[H^+]_o$. The expression was derived by Smith (1987).

1990) may exhibit conductance maxima at PDs far removed from the pump reversal potential. The continuing activity of the proton pump in the high pH state seems rather pointless from a practical point of view. However, the process is not likely to be detrimental to the cell as long as ATP supply is not low.

In a recent article Fisahn and Lucas (1990) describe a collapse and subsequent inversion of extracellular current pattern as *Chara* cells are exposed to high pH. It might be interesting to correlate this phenomenon to the *I/V* profiles. It is possible that the low *G* state corresponds to the collapse of the banding pattern. The inversion of the pattern suggests a pump reactivation (in a different band on the cell) and reappearance of the conductance maximum in the *I/V* profile.

What Ion Carries the Current in High pH state?

While we were not able to provide an answer here, we suggest a possible method involving the patch-clamp technique. Using Fig. 2, the resting PDs and conductances have been tabulated at a range of pH values (*see* Table 3). To estimate the conductance due to the high pH channels, we have to make some assumptions about the other transport systems in the membrane and their behavior in the pH range 7.5 to 12. Bisson (1986) found that the high pH channels are inhibited by darkness. The resting potential and conductance then remain relatively constant in the pH range 7.5–12.0 at levels slightly lower than those at pH 7.5 in the light. Beilby (1984, 1986*b*) found that the conductance maximum due to the pump remains relatively stationary with respect to the membrane PD, as the pH rises. The other major conductance due to K^+ is likely to decline at high pH (Smith et al., 1987). Thus subtracting the conductance profile at pH 7.5 from the higher pH conductances should primarily give us the conductance due to the high pH channels (*see* Table 3). The permeability due to H^+ ions, P_H, or to OH^- ions, P_{OH}, can now be calculated employing an equation derived by Smith (1987), using constant field approximation, and assuming all the conductance increase is due to one or the other. The resultant P_H and P_{OH} can be seen in Table 3; the former increasing by several orders of magnitude, and the latter remaining fairly steady. P_H is rather large compared to other permeabilities, such as P_K (e.g., Hope & Walker, 1975; Smith et al., 1987; Beilby, 1990*b*) or P_{Na} (Hoffmann, Tufariello & Bisson, 1989). This situation arises due to low concentration of H^+. Bisson and Walker (1980) commented on this fact, when they calculated the ratio of P_K/P_H. They also speculated whether there are sufficient H^+ to carry the observed currents and invoked water splitting due to high electric fields (Simons, 1979). Thus these considerations alone are not sufficient to eliminate one of the two types of carriers.

Fortunately, the patch-clamp technique might provide further information. What do the P_H and P_{OH} trends mean in terms of channel populations?

As H^+ ions become scarce, the unitary-channel currents will become smaller and so the H^+ channel population or the open probability of the existing channels must increase sharply to account for the great increase of the conductance at pH 10–11.5. On the other hand, an increase in OH^- will give larger single-channel currents and the channel population and its open probability may remain relatively constant and still generate an increase in conductance. Thus patch-clamp experiments should decisively distinguish the ion responsible for the pH state.

Further, while the picture of constant P_{OH} is appealing in its simplicity, a variable P_H may provide a more powerful model for the banding phenomenon. If the high pH state is taken to be a good model for the membrane underlying the alkaline band, which can have a pH of 10.5 or higher (Fisahn & Lucas, 1990), a constant P_{OH} can explain the maintenance of the alkaline band but not its formation. Consider, for instance, a cell that has been illuminated after a period in the dark. The cytoplasmic pH rises (it had decreased in the dark—Smith, 1984), but probably not high enough to cause substantial rise in G_{OH}, especially since the cytoplasm was found to have a large buffering capacity at high pH (Takeshige & Tazawa, 1989). It is therefore more likely that the H^+ channels open, perhaps in response to rise in cytoplasmic pH (Bisson, 1986). H^+ channels have been isolated from plants previously, and they are incorporated in the ATP synthases in the membranes of chloroplasts (Wagner, Apley & Hanke, 1989).

Another interesting feature of Table 3 is the decrease in conductance at pH 12, although this was not always observed (Bisson & Walker, 1981; Bisson, 1986). If H^+ is the permeant ion, this effect might be explained by its extremely low concentration. Another possibility to consider was the increasing concentration of Na^+. In case of a maxi-K^+ channel this ion acts as a blocker (e.g., Beilby, 1986*a*; Smith et al., 1987; Tester, 1988; Kourie & Findlay, 1990).

Figure 5 shows some of the rather perplexing effects of high Na^+ concentration at pH 10.5. In Fig. 5*A* and *B* the conductance of a fragment was increased by 10 mM Na^+, but APW of pH 12 (made up with 20 mM NaOH) decreased the conductance substantially. When the experiment was repeated adding 20 mM Na^+ to pH 10.5, subsequent pH 12 resulted in a smaller decrease in conductance. The higher conductance of the second *I/V* profile (curve *4*) can be explained by the persistence of the Na^+ effect, even when the Na^+ was removed (possibly we did not succeed in washing it out completely from the wall). However, the conductance decreased at pH 12 even when the Na^+ concentration was kept constant. Figure 5*C* and *D* shows that at 5 mM Na^+ the effects on the *I/V* curve at pH 10.5 are lost in the scatter of the high pH state. In this intact cell the exposure to 20 mM Na^+ caused a considerable decrease in conductance. However, the conductance increased when the cell was bathed in APW of pH 11.5 (made up with 7 mM NaOH). At present we do not know why in some cells the exposure to high Na^+ at pH 10.5 makes the membrane more conductive and in others less conductive. However, in either case the effect of Na^+ seems diminished at very high pH (11.5 and 12) and the decrease of conductance at pH 12 (or the increase of conductance at pH 11.5) is not caused by high Na^+.

The inward rectifier (Cl^- channels) is activated by high Na^+ as observed by Kourie and Findlay (1990). Again, this effect is also diminished by very high pH, but could explain why Tyerman et al. (1986*b*) observed activation of the inward rectifier at more hyperpolarized potentials with increasing pH, while we recorded the opposite trend. The effect of Na^+ certainly requires more experiments.

Excitation

Figures 6 and 7 show that the shape of the AP is essentially conserved regardless of the pH. However, some differences become obvious when we look at the transient currents under voltage-clamp conditions (*see* Fig. 8 and Table 1). It is immediately apparent that the large transient currents at more hyperpolarized PD levels near the threshold of excitation are strongly inhibited by pH 11–11.5, but recover quickly once the neutral pH returns. The currents at more positive PD levels are not as greatly affected, but the recovery is slower. Very similar behavior is observed when the cell PD is held more depolarized with the voltage clamp (Fig. 10 and Table 2). At high pH the cells are damaged by voltage clamping the cell PD for longer periods (minutes) at levels other than the resting potential. Thus to untangle the effect of depolarization and pH is difficult. It may be possible to do so, if we can elicit excitation in a cell, which shows a strong hyperpolarization at pH 11.5 (such as the inexcitable fragment in Fig. 3), but we did not find such a cell in the course of our experiments. Also, as mentioned in Results, clamping to excitable PD levels seems to depolarize the cell's resting PD. However, Fig. 10 indicates that increasing pH does seem to compound the effect of depolarization, as the widening and flattening of the transients is progressively greater at high pH (Fig. 11*D*), although the resting PD passes through a minimum at pH 9.5. Interestingly, low pH combined with low resting PD (Fig. 11*E*) also

diminished the magnitude of the transient conductance.

While the excitation currents are complicated functions of time and PD, the AP shape was observed to reflect their behavior (consider, for instance the effect of temperature and *compare* Figs. 1 and 5 of Beilby & Coster, 1976). However, there is one important difference between the effect of temperature and pH: the temperature influences the excitation currents at all PD levels (*see* Fig. 1 of Beilby & Coster, 1979*b*), whereas pH mainly prolongs the rise time and decreases magnitude of the currents near the excitation threshold. The decay time is very similar regardless of pH or PD (*see* Table 1). It is thus necessary to depolarize the cells further to elicit an AP at high pH (*see* Fig. 7). Subsequently the time dependence of the current at more positive PD levels and at long times is not strongly pH dependent and the AP shapes are similar.

The unusual shape of the AP in Fig. 6*C* and *D* is due to transient opening of the K^+ channels (e.g., Bisson, 1984; Beilby, 1985) upon depolarization. At 2 mM KCl in the medium the K^+ conductance is similar to the pump conductance and the long "shoulder" arises from the pump slowly pulling the membrane potential to more hyperpolarized levels and thus closing the K^+ channels. If the KCl concentration was increased, the K^+ conductance would become greater and the cell would then remain in the K^+ state. At high pH the shoulder becomes a secondary peak, as at high pH the K^+ channels turn on much more slowly (*see* Fig. 7 from Beilby, 1986*b*). Beilby (1986*b*) found that K^+ channels can be activated by depolarization (via voltage clamp) if the high pH APW has also high K^+ concentration. However, either the K^+ or the H^+ (OH^-) channels dominate the membrane conductance. It is understandable that the K^+ channels shut when the membrane is hyperpolarized to E_H, but it is not clear why H^+ channels close in K^+ state as they are only mildly inhibited by depolarization. The interaction of the high pH state and the K^+ state at the time of excitation would be interesting to examine under voltage-clamp conditions. The cell cultures in Sydney, however, display unstable K^+ state (Beilby, 1989*b*), which would make the results too difficult to interpret.

The effect of pH on the transient currents of *Chara* excitation is difficult to analyze in detail, as the picture of excitation has changed considerably in the past few years. The activation and inactivation of the Cl^- current are now assumed to be generated by the rise and fall of Ca^{2+} concentration in the cytoplasm (Lunevsky et al., 1983; Kataev, Zherelova & Berestovsky, 1984; Tsutsui et al., 1986; Shiina & Tazawa, 1987*b*, 1988). In *Nitellopsis* the Cl^- current is indeed preceded by a sharp transient in both free-running AP (Findlay, 1970) and under voltage clamp (Kataev et al., 1984). This transient responds to Ca^{2+} channel blockers. In *Chara* there are often two (or more) current maxima if the plasmalemma is clamped near the threshold PD. The first transient is often of large magnitude (Beilby & Coster, 1979*a*), but as the PD level is made more depolarized (−80 mV), the transient usually shows only one peak and no discernible Ca^{2+} spike can be seen to precede it. (e.g., Fig. 8*A* and *C*). Thus if there is a Ca^{2+} inflow, it is not easily detectable by electrical means. One possibility is a steady Ca^{2+} current rising upon depolarization and remaining at the same level until the PD is returned to the resting level. Experiments with Ba^{2+} (which blocks excitation in *Chara*) suggest that such a current exists (M.J. Beilby, *in preparation*). The level of Ca^{2+} in the cytoplasm would then steadily rise until activation of sequestering mechanisms, which are known to exist (Hayama & Tazawa, 1980). The second peak often observed in the transient current could be due to activation of Cl^- and/or Ca^{2+} channels at the tonoplast (Lunevsky et al., 1983) as the elevated Ca^{2+} reaches it.

It is interesting that at high pH or depolarized (preclamped) PDs multiple current (and conductance) peaks develop at PD levels, where they are not observed in pump state (Figs. 8*B*, 10*C* and 11*B–D*). Perhaps high pH and long-time depolarization affect the dynamics of the Ca^{2+} channels and it takes longer for the Ca^{2+} concentration in the cytoplasm to elevate to the level sufficient to open the Cl^- channels and to reach the tonoplast. Clearly, the excitation in *Chara* needs to be re-examined.

Conclusion

The *I/V* curves measured over the high pH window enabled us to calculate P_H and P_{OH} over this pH range. Translated into the channel population behavior, these should be sufficiently different to allow the patch-clamp technique to distinguish the permeant ion.

The cells remain excitable at high pH, and the shape of the AP is similar to that in the pump state, but the transient currents, while the cell is clamped to excitable PD levels near the excitation threshold, show marked flattening and increase in rise time. Such an effect can be invoked by both pH increase and prolonged depolarization.

The present study suggests a number of future experiments. The patch clamp of the plasmalemma at high pH is the most obvious one. *I/V* and *G/V* profiles of the membrane at high pH in the dark will

provide the behavior of the pump at high pH, which will be valuable for the pump modeling. The effect of high Na^+ concentration needs to be further examined. The excitation-clamp currents should be re-examined with a perturbation sine wave of greater frequency than 5 Hz (Beilby & Beilby, 1983) to distinguish whether there may be a fast Ca^{2+} transient.

The authors would like to thank Prof. N.A. Walker and Dr. D.R. Laver for critical reading of the manuscript. MJB is also indebted to the Australian Research Council for funding this research via grant to Prof. Walker. Some of the results were presented at the 12th scientific meeting of the Australian Society for Biophysics in Armidale, Australia, 1988; and at Symposium on Ion Transport, Okazaki, Japan, 1991.

References

Beilby, M.J. 1984. Current-voltage characteristics of the proton pump at *Chara* plasmalemma: I. pH dependence. *J. Membrane Biol.* **81:**113–125

Beilby, M.J. 1985. Potassium channels at *Chara* plasmalemma. *J. Exp. Bot.* **36:**228–239

Beilby, M.J. 1986*a*. Factors controlling the K^+ conductance in *Chara*. *J. Membrane Biol.* **93:**187–193

Beilby, M.J. 1986*b*. Potassium channels and different states of *Chara* plasmalemma. *J. Membrane Biol.* **89:**241–249

Beilby, M.J. 1989*a*. Electrophysiology of giant algal cells. *In:* Methods in Enzymology. S. Fleischer and B. Fleischer, editors. Vol. 174, pp. 403–443. Academic, San Diego

Beilby, M.J. 1989*b*. K^+ state in different charophyte cultures. 13th Scientific Meeting of the Australian Society for Biophysics, Adelaide, Australia

Beilby, M.J. 1990*a*. Current-voltage curves for plant membrane studies: A critical analysis of the method. *J. Exp. Bot.* **41:**165–182

Beilby, M.J. 1990*b*. The *I/V* technique and the different states of *Chara* plasmalemma. *In:* Membrane Transport in Plants and Fungi. M.J. Beilby, N.A. Walker, and J.R. Smith, editors. pp. 61–66. University of Sydney Press, Sydney

Beilby, M.J., Beilby, B.N. 1983. Potential dependence of the admittance of *Chara* plasmalemma. *J. Membrane Biol.* **74:**229–245

Beilby, M.J., Coster, H.G.L. 1976. The action potential in *Chara corallina:* Effect of temperature. *Aust. J. Plant Physiol.* **3:**275–289

Beilby, M.J., Coster, H.G.L. 1979*a*. The action potential in *Chara corallina*. II. Two activation-inactivation transients in voltage clamps of the plasmalemma. *Aust. J. Plant Physiol.* **6:**323–335

Beilby, M.J., Coster, H.G.L. 1979*b*. The action potential in *Chara corallina*. IV. Activation enthalpies of the Hodgkin-Huxley gates. *Aust. J. Plant Physiol.* **6:**355–365

Beilby, M.J., Shepherd, V.A. 1989. Cytoplasm-enriched fragments of *Chara:* Structure and electrophysiology. *Protoplasma* **148:**150–163

Bisson, M.A. 1984. Calcium effects on electrogenic pump and passive permeability of the plasma membrane of *Chara corallina*. *J. Membrane Biol.* **81:**59–67

Bisson, M.A. 1986. The effect of darkness on active and passive transport in *Chara corallina*. *J. Exp. Bot.* **37:**8–21

Bisson, M.A., Bartholomew, D. 1988. Osmoregulation or turgor regulation in *Chara? Plant Physiol.* **74:**252–255

Bisson, M.A., Walker, N.A. 1980. The *Chara* plasmalemma at high pH. Electrical measurements show rapid specific passive uniport of H^+ or OH^- *J. Membrane Biol.* **56:**1–7

Bisson, M.A., Walker, N.A. 1981. The hyperpolarization of the *Chara* membrane at high pH: Effects of external potassium, internal pH, and DCCD. *J. Exp. Bot.* **32:**951–971

Bisson, M.A., Walker, N.A. 1982. Control of passive permeability in the *Chara* plasmalemma. *J. Exp. Bot.* **33:**520–532

Blatt, M.R., Beilby, M.J., Tester, M. 1990. Voltage dependence of the *Chara* proton pump revealed by current-voltage measurement during rapid metabolic blockade with cyanide. *J. Membrane Biol.* **114:**205–223

Coleman, H.A. 1986. Chloride currents in *Chara*—a patch clamp study. *J. Membrane Biol.* **93:**55–61

Findlay, G.P. 1970. Membrane electrical behaviour in *Nitellopsis obtusa*. *Aust. J. Biol. Sci.* **23:**1033–1045

Fisahn, J., Lucas, W.J. 1990. Inversion of extracellular current and axial voltage profile in *Chara* and *Nitella*. *J. Membrane Biol.* **113:**23–30

Gradmann D. 1989. Use and misuse of patch clamp in plant physiology. *In:* Plant Membrane Transport: The Current Position. J. Dainty, M.I. DeMichelis, E. Marre, and F. Rasi-Caldogno, editors. pp. 513–516. Elsevier, Amsterdam—New York—Oxford

Hansen, U.-P., Gradmann, D., Sanders, D., Slayman, C.L. 1981. Interpretation of current-voltage relationships for "active" ion transport systems: I. Steady-state reaction-kinetic analysis of class-I mechanisms. *J. Membrane Biol.* **63:**165–190

Hayama, T., Tazawa, M. 1980. Ca^{2+} reversibly inhibits rotation of chloroplasts in isolated cytoplasmic droplets of *Chara*. *Protoplasma* **102:**1–9

Hoffmann, R., Tufariello, J., Bisson, M.A. 1989. Effect of divalent cations on Na^+ permeability of *Chara corallina* and freshwater grown *Chara buckellii*. *J. Exp. Bot.* **40:**875–881

Hope, A.B., Walker, N.A. 1975. The Physiology of Giant Algal Cells. Cambridge University Press, London

Kataev, A.A., Zherelova, O.M., Berestovsky, G.N. 1984. Ca^{2+}-induced activation and irreversible inactivation of chloride channels in the perfused plasmalemma of *Nitellopsis obtusa*. *Gen. Physiol. Biophys.* **3:**447–462

Kourie, J.I., Findlay, G.P. 1990. Ionic currents across the membranes of *Chara inflata* cells. II. Effects of external Na^+, Ca^{2+} and Cl^- on K^+ and Cl^- currents. *J. Exp. Bot.* **41:**151–163

Laver, D. R. 1991. A surgical method for accessing the plasmalemma. *Protoplasma* **161:**79–84

Lucas, W.J. 1982. Mechanism of acquisition of exogenous bicarbonate by internodal cells of *Chara corallina*. *Planta* **156:**181–192

Lucas, W.J. 1985. Bicarbonate utilization by *Chara:* A reanalysis. *In:* Inorganic Carbon Uptake by Aquatic Photosynthetic Organisms. W.J. Lucas and J.A. Berry, editors. pp. 223–254. American Society of Plant Physiologists, Rockville (MD)

Lucas, W.J., Shimmen, T. 1981. Intracellular perfusion and cell centrifugation studies on plasmalemma transport processes in *Chara corallina*. *J. Membrane Biol.* **58:**227–237

Lunevsky, V.Z., Zherelova, O.M., Vostrikov, I.Y., Berestovsky, G.N. 1983. Excitation of *Characeae* cell membranes as a result of activation of calcium and chloride channels. *J. Membrane Biol.* **72:**43–58

Price, G.D., Badger, M.R. 1985. Inhibition by proton buffers of photosynthetic utilization of bicarbonate in *Chara corallina*. *Aust. J. Plant Physiol.* **12:**257–267

Prins, H.B.A., Snell, J.F.H., Helder, R.J., Zanastra, P.E. 1980. Photosynthetic HCO_3^- utilization and OH^- excretion in

aquatic angiosperms. Light induced pH changes at the leaf surface. *Plant Physiol.* **66:**818–822

Raven, J.A. 1991. Terrestrial rhizophytes and H^+ currents circulating over at least a millimetre: An obligate relationship? *New Phytol.* **117:**177–185

Reid, R.J., Smith, F.A. 1988. Measurements of the cytoplasmic pH of *Chara corallina* using double-barreled pH microelectrodes. *J. Exp. Bot.* **39:**1421–1432

Shepherd, V.A., Goodwin, P.B. 1991. Seasonal patterns of behaviour in *Chara corallina* Klein ex Wild. I. Cell-cell communication in vegetative lateral branches during winter. *Plant, Cell Environ. (in press)*

Shiina, T., Tazawa, M. 1987*a*. Ca^{2+}-activated Cl^- channel in plasmalemma of *Nitellopsis obtusa*. *J. Membrane Biol.* **99:**137–146

Shiina, T., Tazawa, M. 1987*b*. Demonstration and characterisation of Ca^{2+} channel in tonoplast-free cells of *Nitellopsis obtusa*. *J. Membrane Biol.* **96:**263–276

Shiina, T., Tazawa, M. 1988. Ca^{2+}-dependent Cl^- efflux in tonoplast-free cells of *Nitellopsis obtusa*. *J. Membrane Biol.* **106:**135–139

Simons, R. 1979. Strong electric field effects on proton transfer between membrane-bound amines and water. *Nature* **280:**824–826

Smith, F. A. 1984. Regulation of cytoplasmic pH of *Chara corallina:* Response to changes in external pH. *J. Exp. Bot.* **35:**43–50

Smith, J.R. 1987. Potassium transport across the membranes of *Chara*. II. ^{42}K fluxes and the electrical current as a function of membrane voltage. *J. Exp. Bot.* **38:**752–777

Smith, J.R., Walker, N.A., Smith, F.A. 1987. Potassium transport across the membranes of *Chara*. III. Effects of pH, inhibitors and illumination. *J. Exp. Bot.* **38:**778–787

Takeshige, K., Tazawa, M. 1989. Measurement of the cytoplasmic and vacuolar buffer capacities in *Chara corallina*. *Plant Physiol.* **89:**1049–1052

Tester, M. 1988. Blockade of potassium channels in the plasmalemma of *Chara corallina* by tetraethylammonium, Ba^{2+}, Na^+ and Cs^+. *J. Membrane Biol.* **105:**77–85

Tsutsui, I., Ohkawa, T., Nagai, R., Kishimoto, U. 1986. Inhibition of the Cl^- channel activation in *Chara corallina* membrane by lanthanum ion. *Plant Cell Physiol.* **27:**1197–1200

Tyerman, S.D., Findlay, G.P., Paterson, G.J. 1986*a*. Inward membrane current in *Chara inflata:* I. A voltage- and time-dependent component. *J. Membrane Biol.* **89:**139–152

Tyerman, S.D., Findlay, G.P., Paterson, G.J. 1986*b*. Inward membrane current in *Chara inflata:* II. Effects of pH, Cl^--channel blockers and NH_4^+, and significance for the hyperpolarized state. *J. Membrane Biol.* **89:**153–161

Wagner, R., Apley, E.C., Hanke, W. 1989. Single channel H^+ currents through reconstituted chloroplast ATP synthase CF_0–CF_1. *EMBO J.* **8:**2827–2834

Walker, N.A., Smith, F.A., Cathers, I.R. 1980. Bicarbonate assimilation by freshwater charophytes and higher plants: I. Membrane transport of bicarbonate ions is not proven. *J. Membrane Biol.* **57:**51–58

Received 30 November 1990; revised 15 July 1991